# Model-independent source imaging using two-pion correlations in 2 to 8$A$ GeV Au + Au collisions

S.Y. Panitkin,[7] N.N. Ajitanand,[12] J. Alexander,[12] M. Anderson,[5] D. Best,[1] F.P. Brady,[5] T. Case,[1] W. Caskey,[5] D. Cebra,[5] J. Chance,[5] P. Chung,[12] B. Cole,[4] K. Crowe,[1] A. Das,[10] J. Draper,[5] M. Gilkes,[11] S. Gushue,[2] M. Heffner,[5] A. Hirsch,[11] E. Hjort,[11] L. Huo,[6] M. Justice,[7] M. Kaplan,[3] D. Keane,[7] J. Kintner,[8] J. Klay,[5] D. Krofcheck,[9] R. Lacey,[12] M.A. Lisa,[10] H. Liu,[7] Y.M. Liu,[6] R. McGrath,[12] Z. Milosevich,[3], G. Odyniec,[1] D. Olson,[1] C. Pinkenburg,[12] N. Porile,[11] G. Rai,[1] H.G. Ritter,[1] J. Romero,[5] R. Scharenberg,[11] L.S. Schroeder,[1] B. Srivastava,[11] N.T.B. Stone,[2] T.J.M. Symons,[1] S. Wang,[7] J. Whitfield,[3] T. Wienold,[1] R. Witt,[7] L. Wood,[5] X. Yang,[4] W.N. Zhang,[6] Y. Zhang [4]
(E895 Collaboration)
and D.A. Brown[13], P. Danielewicz[14]

[1]*Lawrence Berkeley National Laboratory, Berkeley, California 94720*
[2]*Brookhaven National Laboratory, Upton, New York 11973*
[3]*Carnegie Mellon University, Pittsburgh, Pennsylvania 15213*
[4]*Columbia University, New York, New York 10027*
[5]*University of California, Davis, California 95616*
[6]*Harbin Institute of Technology, Harbin 150001, P. R. China*
[7]*Kent State University, Kent, Ohio 44242*
[8]*St. Mary's College of California, Moraga, California 94575*
[9]*University of Auckland, Auckland, New Zealand*
[10]*The Ohio State University, Columbus, Ohio 43210*
[11]*Purdue University, West Lafayette, Indiana 47907*
[12]*State University of New York, Stony Brook, New York 11794*
[13]*University of Washington, Seattle, Washington 98195*
[14]*Michigan State University, East Lansing, Michigan 48824*

(April 5, 2000)

We report a particle source imaging analysis based on two-pion correlations in high multiplicity Au + Au collisions at beam energies between 2 and 8$A$ GeV. We apply the imaging technique introduced by Brown and Danielewicz, which allows a model-independent extraction of source functions with useful accuracy out to relative pion separations of about 20 fm. The extracted source function have Gaussian shapes. Imaging results are found to be consistent with conventional source parameters obtained from a multidimensional HBT analysis. Measurements indicate substantial expansion of the pion source. However effective volumes are almost constant across the energy range under study.

One of the robust predictions of Quantum Chromodynamics is that strongly interacting matter can exist in a state with colored degrees of freedom, i.e., quarks and gluons, if subjected to sufficiently high temperature or density [1]. This deconfined state of matter, often called Quark-Gluon Plasma (QGP), may have been present in the Universe a few microseconds after the Big Bang. It is also believed that QGP can be produced in collisions of heavy ions at high energies. Experimental searches for evidence of QGP are prominent and challenging priorities in modern heavy-ion physics. A major difficulty is that the sought-after QGP is a transient state which persists only for timescales on the order of fm/$c$. After expansion and cooling, any QGP necessarily undergoes a phase transition to hadronic matter, possibly leaving little evidence behind in the final state of the collision. Numerous experimental observables have been proposed as signatures of QGP creation in heavy-ion collisions [2]. One of the more promising of these is based on the expectation that the larger number of degrees of freedom associated with the deconfined state should manifest itself in increased system entropy, which ought to survive subsequent hadronization and freeze-out. The specific prediction is that QGP formation will cause the system to expand more and/or interact for a longer time and produce more particles, relative to a system which remained in the hadronic phase throughout the collision process.

Intensity interferometry [3] has been extensively used to extract information about spatial-temporal properties of heavy-ion collisions. The HBT approach [3–8] is well understood from the theoretical point of view, and is the mainstream analysis method for meson $(\pi, K)$ intensity interferometry. A novel approach — the imaging technique introduced by Brown and Danielewicz [9–11] — offers the opportunity to use *any* class of like-pair correlations to reconstruct the entire source function, as opposed to the conventional model-dependent parametrization. The two approaches have natural connections, which are especially clear for the case of non-interacting spin-zero bosons [12]. In this paper, we report the first application of the source imaging technique to experimental data, specifically negative pions from Au + Au collisions at beam energies between 2 and 8$A$ GeV, with particular emphasis on verification and study of the expected connection with the source parameters obtained from HBT analysis. Comparing the two methods not only allows us to test the model underlying the HBT parametrization, but also lends credibility to the source imaging approach in other contexts such as proton-proton correlations, where the HBT technique cannot be applied.

We present data from experiment E895 [14], in which Au beams of kinetic energy 1.85, 3.9, 5.9 and 7.9$A$ GeV from the AGS accelerator at Brookhaven were incident on a fixed Au target. The analyzed $\pi^-$ samples come from the main E895 subsystem — the EOS Time Projection Chamber (TPC) [15], located in a dipole magnetic field of 0.75 or 1.0 Tesla. Results of the E895 $\pi^-$ HBT analysis were reported earlier [16], and in this Letter, we focus on an application of the imaging to the same datasets.

In order to obtain the two-pion correlation function $C_2$ experimentally, the standard event-mixing technique was used [17]. Before calculating the correlation functions, several cuts were applied, identical to those used in our earlier HBT analysis [16]. Negative pions were detected and reconstructed over a substantial fraction of $4\pi$ solid angle in the center-of-mass frame, and simultaneous measurement of particle momentum and specific ionization in the TPC gas helped to separate $\pi^-$ from other negatively charge particles, such as electrons, $\mathrm{K}^-$ and antiprotons. Contamination from these species is estimated to be under 5%, and is even less at the lower beam energies and higher transverse momenta. Momentum resolution in the region of correlation measurements is better than 3%. Event centrality selection was based on the multiplicity of reconstructed charged particles. In the present analysis, events were selected with a multiplicity corresponding to the upper 11% of the inelastic cross section for Au + Au collisions. Only pions with $p_T$ between 100 MeV/$c$ and 300 MeV/$c$ and within $\pm 0.35$ units from midrapidity were used, and each track was required to consist of 20 or more hits in the TPC. The latter criterion suppresses short tracks from $\delta$-electrons and from remnants of split tracks. Another requirement was for each used $\pi^-$ track to point back to the primary event vertex with a distance of closest approach (DCA) less than 2.5 cm. This cut removes most pions originating from weak decays of long-lived particles, e.g. $\Lambda$ and $\mathrm{K}^0$. Monte Carlo simulations based on the RQMD model [18] indicate that decay daughters are present at a level that varies from 5% at 4$A$ GeV to 10% at 8$A$ GeV, and they lie preferentially at $p_T < 100$ MeV/$c$. Finally, in order to overcome effects of track merging, a cut on spatial separation of two tracks was imposed. For pairs from both "true" and "background" distributions, the separation between two tracks was required to be greater than 4.5 cm over a distance of 18 cm in the beam direction. This cut also suppresses effects of track splitting [16].

Imaging [9,10] was used to extract quantitative information from the measured correlation functions. It has been shown [11] that imaging allows robust reconstruction of the source function for systems with non-zero lifetime, even in the presence of strong space-momentum correlations. The main features of the method are outlined below; see Refs [9,10,12] for more details. The two-particle correlation function may be expressed as follows:

$$C_{\mathbf{P}}(\mathbf{Q}) \simeq \int d\mathbf{r}\, |\Phi^{(-)}_{\mathbf{Q}}(\mathbf{r})|^2\, S_{\mathbf{P}}(\mathbf{r}) \tag{1}$$

$S_{\mathbf{P}}(\mathbf{r})$ is the distribution of relative separation of emission points for the two particles in their center-of-mass frame, and $\Phi^{(-)}_{\mathbf{Q}}(\mathbf{r})$ is a relative wave function. The total momentum of the pair is denoted by $\mathbf{P}$, the relative momentum by $\mathbf{Q} = \mathbf{p_1} - \mathbf{p_2}$, and the relative separation by $\mathbf{r}$. In the identical noninterecting pion case, the relative wave function can be expressed as

$$\Phi^{(-)}_{\mathbf{Q}}(\mathbf{r}) = \frac{1}{\sqrt{2}} \left( e^{i\mathbf{Q}/2\cdot\mathbf{r}} + e^{-i\mathbf{Q}/2\cdot\mathbf{r}} \right). \tag{2}$$

The goal of imaging is the determination of the relative source function ($S_{\mathbf{P}}(\mathbf{r})$ in Eq. (1)), given $C_{\mathbf{P}}(\mathbf{Q})$. Since the nontrivial part of the correlation function is its deviation from unity, one may rewrite Eq. 1 as

$$C_{\mathbf{P}}(\mathbf{Q}) - 1 = \int d\mathbf{r}\, K(\mathbf{Q},\mathbf{r})\, S_{\mathbf{P}}(\mathbf{r}), \tag{3}$$

where $K = |\Phi^{(-)}_{\mathbf{Q}}(\mathbf{r})|^2 - 1$. The problem of imaging then reduces to the problem of inverting [20] $K(\mathbf{q},\mathbf{r})$ in Eq. (3). For pions, one might think that because Eq. 1 (or 3) is a Fourier cosine transform it may be inverted analytically [9] to give the source function directly in terms of the correlation function:

$$S_{\mathbf{p}}(\mathbf{r}) = \frac{1}{(2\pi)^3} \int d^3Q\, \cos(\mathbf{Q}\cdot\mathbf{r})\, (C_{\mathbf{p}}(\mathbf{Q}) - 1). \tag{4}$$

While this might work for vanishing experimental uncertainty, for realistic situations this is a poor way to perform the inversion. When Fourier transforming, it is impossible to distinguish between statistical noise and real structure in the data. Furthermore, the errors on the source that one obtains from straightforward error propagation in this method do not accurately reflect the true uncertainty in the source [21].

Instead, we proceed as in [9,10] discretize either Eq. (3) to obtain the matrix equation $C_i = \sum_j K_{ij} S_j$. Imaging reduces to finding the set of source points, $S_j$, that minimize the $\chi^2$. Here, $\chi^2 = \sum_i (C_i - \sum_j K_{ij} S_j)^2/\Delta^2 C_i$. This source is $S_j = \sum_i [(K^T B K)^{-1} K^T B]_{ji} (C_i - 1)$ where $K^T$ is the transpose of the kernel matrix and $B$ is the inverse covariance matrix of the data $B_{ij} = \delta_{ij}/\Delta^2 C_i$. The uncertainty of the source is the square-root of the diagonal elements of the covariance matrix of the source, $\Delta^2 S = (K^T B K)^{-1}$.

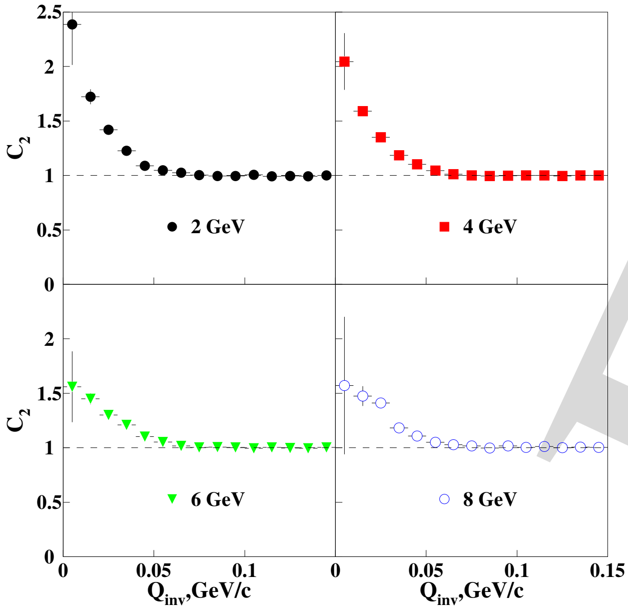


FIG. 1. Measured two-pion correlation functions for Au + Au central collisions at four beam energies.

It has been shown [12] that for the case of noninteracting spin-zero bosons with Gaussian correlations, there is a natural connection between the imaged sources and "standard" HBT parameters. Indeed, the source is a Gaussian with the "standard" HBT parameters as radii:

$$S(\mathbf{r}) = \frac{\lambda}{(2\sqrt{\pi})^3\sqrt{\det{[R^2]}}} \exp\left(-\frac{1}{4} r_i r_j [R^2]^{-1}_{ij}\right), \quad (5)$$

where $\lambda$ is a fit parameter traditionally called the chaoticity or coherence factor in HBT analyses. Here, $[R^2]$ is the real symmetric matrix of radius parameters

$$[R^2] = \begin{pmatrix} R_o^2 & R_{os}^2 & R_{o\ell}^2 \\ R_{os}^2 & R_s^2 & R_{s\ell}^2 \\ R_{o\ell}^2 & R_{s\ell}^2 & R_\ell^2 \end{pmatrix}. \quad (6)$$

Eq. (7) is the most general Gaussian one may use, but usually one assumes a particular symmetry of the single particle source so that there is only one non-vanishing non-diagonal element $R_{ol}^2$. The asymptotic value of the relative source function at zero separation $S(\mathbf{r} \to 0)$ has the meaning of the inverse effective volume of particle emission, and has units of fm$^{-3}$:

$$S(\mathbf{r} \to 0) = \frac{\lambda}{(2\sqrt{\pi})^3\sqrt{\det{[R^2]}}}. \quad (7)$$

This effective volume is an important parameter needed to extract the space averaged phase-space density.

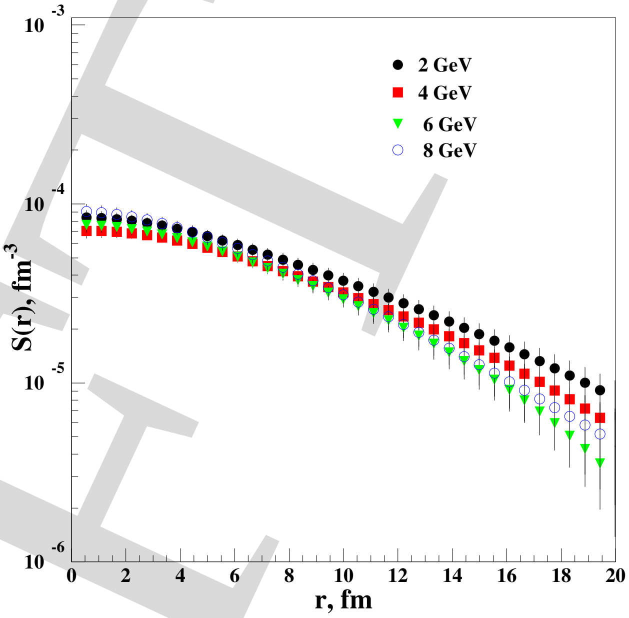


FIG. 2. Relative source functions extracted from the pion correlation data at 2, 4, 6 and 8$A$ GeV.

Figure 1 shows measured angle averaged two-pion correlation functions for central Au + Au collisions at 2, 4, 6 and 8$A$ GeV. Figure 2 shows relative source functions $S(r)$ obtained by applying the imaging technique to the measured two-pion correlation functions. The plotted points are not statistically independent of each other, and were obtained from expansion of the source functions using basis splines [22]. With this technique, we may reconstruct the distribution of relative pion separations with useful accuracy out to $r \sim 20$ fm. The images obtained at each of the four E895 beam energies are rather similar in shape, and upon fitting with a Gaussian function , values of $\chi^2$ per degree of freedom between 0.9 and 1.2 are obtained. Results of fits to the source function and correlation functions are shown in Table I. One can see that source radii extracted via both techniques are similar, further confirming the validity of a Gaussian source hypothesis. Figure 3 compares effective volumes of pion emission inferred from the standard Bertsch-Pratt pion HBT parametrization (open circles) with the effective volumes derived from the image source functions shown in Fig. 2 (solid circles).

TABLE I. Radius parameters of Gaussian fits to the extracted source ($R_S$) functions and measured correlation functions($R_{C2}$) for different energies.

| $E_b$ (AGeV) | 2 | 4 | 6 | 8 |
|---|---|---|---|---|
| $R_S$(fm) | 6.70±0.04 | 6.35±0.03 | 5.56±0.03 | 5.53±0.05 |
| $R_{C2}$ (fm) | 6.39±0.2 | 6.05±0.1 | 5.51±0.15 | 5.61±0.28 |

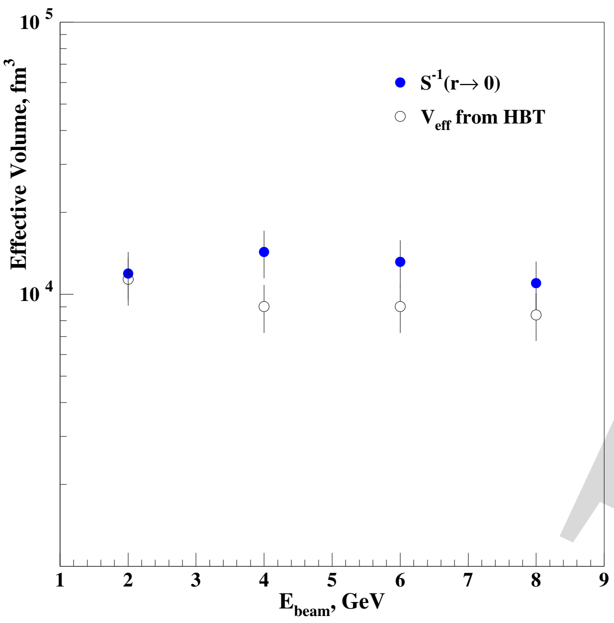


FIG. 3. Effective volumes of pion emission as a function of beam energy, obtained using imaging (solid circles) and HBT (open circles).

Essentially, this figure plots the inverse of the left- and right-hand sides of Eq. 7. Results of the multidimensional Bertsch-Pratt fit to the pion correlation data have already been published in Ref. [16] and are reproduced in Table II. It can be seen from Fig. 3 that the agreement between imaging and the HBT parametrization is within 10%. Figure 3 also demonstrates that the measured volumes of pion emission are about an order of magnitude larger than the volume of a gold nucleus ($\approx 1100 fm^3$), indicating a significant expansion of the emitting source at E895 energies. Effective volumes are constant within errors across the 2 to 8$A$ GeV beam energy range.

In summary, we present measurements of one-dimensional correlation functions for negative pions emitted at mid-rapidity from central Au + Au collisions at 2, 4, 6 and 8$A$ GeV. These correlation functions are analyzed using the imaging technique of Brown and Danielewicz. It is found that relative source functions $S(r)$ have rather similar shapes and zero-separation intercepts $S(r \to 0)$. Distributions of relative separation have been measured out to 20 fm, and the extracted source functions are approximately Gaussian. We have performed the first experimental check of the predicted connection between imaging and traditional meson interferometry techniques and found that the two methods agree within 10%. This agreement paves the way for applications of the imaging method to the interpretation of pair correlations among strongly interacting particle such as protons, antiprotons, etc. Measured volumes of pion emission are about an order of magnitude larger than the volume of a gold nucleus, indicating a substantial expansion of the emitting source. However, effective volumes are almost constant across the 2 to 8$A$ GeV range of bombarding energies under study.

TABLE II. Fit parameters for the Bertsch-Pratt HBT parameterization of the pion correlation functions for E895 beam energies used for calculations of effective volumes.

| $E_b$ (AGeV) | 2 | 4 | 6 | 8 |
|---|---|---|---|---|
| $\lambda$ | 0.99±0.06 | 0.82±0.04 | 0.65±0.03 | 0.65±0.05 |
| $R_o$ (fm) | 6.22±0.26 | 5.94±0.20 | 5.76±0.23 | 5.49±0.31 |
| $R_s$ (fm) | 6.28±0.20 | 5.68±0.14 | 5.05±0.12 | 4.83±0.21 |
| $R_l$ (fm) | 6.51±0.19 | 4.92±0.15 | 4.72±0.18 | 4.64±0.24 |
| $R_{ol}^2$ (fm) | -2.43±1.71 | -1.99±1.22 | 2.17±1.20 | -0.65±1.85 |

Stimulating discussions with Drs. G.F. Bertsch, S. Pratt, S.A. Voloshin and N. Xu are gratefully acknowledged. This research is supported by US DOE, NSF and other funding, as detailed in Ref. [23].

[1] E.V. Shuryak, Phys. Rep **61**, 71 (1980).
[2] B. Muller, nucl-th/9906029
[3] V.G Grishin, G.I. Kopylov and M.I. Podgoretski, Sov. J. Nucl. Phys. **13**, 638 (1971).
[4] S. Pratt, T. Csörgő and T. Zimányi, Phys. Rev. **C42**, 2646 (1990).
[5] C. Gelbke and B.K. Jennings, Rev. Mod. Phys. **62**, 553 (1990).
[6] S. Pratt, Nucl. Phys. **A638**, 125c (1998).
[7] U.A Wiedemann and U. Heinz, nucl-th/9901094
[8] U. Heinz and B. Jacak, nucl-th/9902020, Ann. Rev. Nucl. Part. Sci **49** (1999).
[9] D.A. Brown and P. Danielewicz, Phys. Lett. **B398**, 252 (1997).
[10] D.A. Brown and P. Danielewicz, Phys. Rev. **C57**, 2474 (1998).
[11] S.Y. Panitkin and D.A. Brown, Phys. Rev. **C61**, 021901 (2000).
[12] D.A. Brown, S.Y. Panitkin and G.F. Bertsch, nucl-th/0002039.
[13] D.A. Brown, nucl-th/0003021.
[14] G. Rai *et al.*, proposal LBL-PUB-5399 (1993).
[15] G. Rai *et al.*, IEEE Trans. Nucl. Sci. **37**, 56 (1990).
[16] E895 Collaboration, M.A. Lisa *et al.*, Phys. Rev. Lett. **84**, 2798 (2000).
[17] G. Kopylov, Phys. Lett. **50B**, 472 (1974).
[18] H. Sorge, Phys. Rev. C **52**, 3291 (1995).
[19] W.G.J. Stoks *et al.*, Phys. Rev. **C49**, 2950 (1994).
[20] A. Tarantola, *Inverse Problem Theory*, Elsevier, (1987).
[21] D. Brown, nucl-th/9904063.
[22] D.A. Brown and P. Danielewicz, in preparation; C. de Boor, *A Practical Guide to Splines*, Springer-Verlag, (1978).
[23] E895 Collaboration, P. Chung *et al.*, to be published.